International Journal of Thermophysics, Vol. 23, No. 6, November 2002 (© 2002)

Thermal Radiation Calorimeter for Measuring the Specific Heat Capacity of Liquid Samples

S. Sawai,[1,2] A. Uematsu,[1] K. Morimoto,[1] and K. Hisano[1]

Received March 13, 2002

A new thermal radiation calorimeter for measuring the specific heat capacity of liquid samples continuously in the temperature range from 280 to 360 K is described. The heat input to the sample cell from the heater by thermal radiation is estimated using the effective emissivity, which is the apparatus constant. The heat capacity of a sample can be calculated from the temperatures of the sample and the heater, and the temperature change rate of the sample. The present sample cell was made of Pyrex glass; therefore most liquid samples do not react with the sample cell, and blackening of the surface of the sample cell is not necessary in the present temperature range. The specific heat capacities for ethanol, ethylene glycol, n-heptane, n-valeric acid, and water + ethanol mixtures were measured to confirm the reliability of the present calorimeter.

KEY WORDS: liquid sample; Pyrex glass cell; specific heat capacity; thermal radiation calorimeter.

1. INTRODUCTION

A radiation calorimeter, in which a sample is heated and/or cooled by thermal radiation, has been developed by several authors [1–4]. In these methods, the exact estimation of the heat transfer between the sample and the heater is necessary. In previous papers [5–7], the authors described a new thermal radiation calorimeter for measurement of the specific heat capacity of a solid sample. The principle of this method is based on the net-radiation theory [8, 9]. In this method, a disk-shaped solid sample is heated and cooled only by thermal radiation from a heater in a vacuum

---

[1] Department of Applied Physics, National Defense Academy, Hashirimizu 1-10-20, Yokosuka 239-8686, Japan.

[2] To whom correspondence should be addressed. E-mail: sawai@nda.ac.jp

0195-928X/02/1100-1617/0

chamber. The surfaces of the sample, the heater, and the wall of the independent chamber are blackened with a high emissivity material to keep their emissivities high and constant independent of sample and temperature. The radiant power exchanged between the heater, the sample, and the wall of the chamber is evaluated using the effective emissivity, which is the apparatus constant, and is estimated experimentally with a standard sample having a known heat capacity. The specific heat capacity is obtained only from the temperatures of the sample and the heater, and the time rate change of the sample temperature. This method enables the values of the specific heat to be obtained continuously with temperature in a straightforward manner, and over a wide temperature range. The construction and operation of this apparatus are very simple.

The present paper describes the improvement of this calorimeter to measure the specific heat capacity of a liquid sample and reports the initial measurements. The temperature range was from 280 to 360 K. The sample cell was made of Pyrex glass. Blackening of the surface of the sample cell, which is necessary for the usual thermal radiation calorimeter, is not necessary because the emissivity of Pyrex glass is high and fairly constant in the present temperature range. Pyrex glass is resistant to corrosion from a liquid sample, so most liquids do not become contaminated by the cell. The specific heat capacities of ethanol, ethylene glycol, n-heptane, n-valeric acid, and binary mixtures of ethanol and water were measured, and these values have been compared with those published in the literature to confirm the reliability of the present calorimeter.

2. EXPERIMENTAL

The theory of the thermal radiation calorimeter has already been presented in previous papers [5–7]. When a sample (mass M, surface area A, and heat capacity C_p) is heated only by thermal radiation from a heater in a vacuum chamber, the time rate change of the sample temperature, dT_s/dt, is described by

$$MC_\mathrm{p}\frac{dT_\mathrm{s}}{dt}=E_\mathrm{h}A(I_\mathrm{h}-I_\mathrm{s})-E_\mathrm{s}A(I_\mathrm{s}-I_\mathrm{w})-\frac{dQ_\mathrm{s}}{dt}, \tag{1}$$

where I is the emissive power per unit area of blackbody radiation, which is equal to σT^4 (σ is the Stefan–Boltzmann constant and T is temperature). Subscripts s, h, and w refer to the sample, the heater, and the wall of the vacuum chamber, respectively. dQ_s/dt is the conductive heat loss per unit time through thermocouple leads. E_h and E_s are the *effective emissivities* arising from the radiant heat transfer between the sample, the heater, and the chamber wall. The validity of Eq. (1) is presented in an Appendix. In a typical experimental run, the sample is heated gradually over a certain temperature range and then cooled over the same range. T_w is maintained constant during the experiment. The heat capacity C_p is derived from Eq. (1) at the same sample temperature T_s for the heating process (i) and the cooling process (d):

$$\frac{C_p}{E_h} = \frac{A(I_{hi} - I_{hd})}{M\left\{\left(\frac{dT_s}{dt}\right)_i - \left(\frac{dT_s}{dt}\right)_d\right\}}, \tag{2}$$

where $(dQ_s/dt)_i = (dQ_s/dt)_d$ at the same T_s was assumed. The left-hand side of Eq. (2) can be estimated because all parameters on the right-hand side of Eq. (2) can be measured experimentally. The value measured directly in this method is not C_p but C_p/E_h. However, if E_h is evaluated experimentally with the standard sample having a known heat capacity, the heat capacity $C_p(T_s)$ can be estimated.

A schematic diagram of the present experimental setup and the sample cell is shown in Fig. 1. A sample cell and two plate heaters were set in the vacuum chamber which was evacuated to 10^{-4} Pa during the measurement. The dimensions of the vacuum chamber were 100 mm inside diameter and 200 mm high, and the temperature of the chamber wall was kept at 253.15 K by a refrigerated circulator. The inside wall of the chamber was coated with a mixture of Electrodag188 (Acheson) and glass powders for blackening. Heaters were made with alumina ceramics, and the size of them

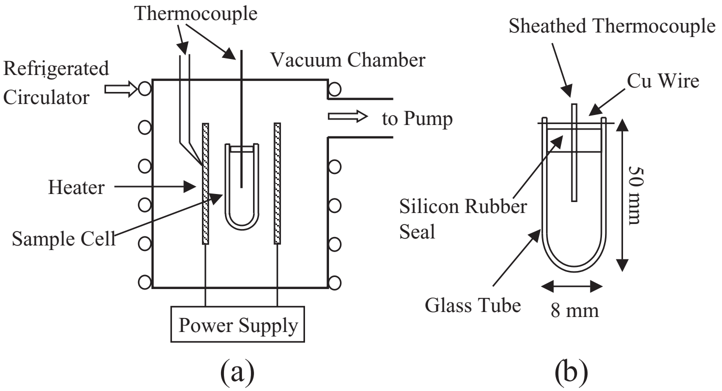

Fig. 1. (a) Cross-sectional schematic diagram of the experimental apparatus. (b) Schematic view of a sample cell.

is 60 × 50 mm, 0.8 mm thick. Their surfaces were coated with a small amount of Electrodag188. The temperature of the heater, T_h, was measured by a chromel-alumel thermocouple (0.1 mm in diameter) which was directly attached to the heater. The sample cell was made of a Pyrex glass tube, 8 mm in inside diameter, 10 mm in outside diameter, and 50 mm in length, which is filled with 2 ml of a liquid sample. The upper end of the tube was sealed with silicon rubber. A copper-constantan thermocouple sheathed in a tube of Inconel 600, 0.5 mm in tube diameter, was inserted into the liquid sample through the hole bored in the silicon rubber seal to measure the sample temperature. The sample cell was suspended only by the sheath of the thermocouple. The time rate change of the sample temperature was from 0.9 to 1.6 $\mathrm{K \cdot min^{-1}}$ in the present measurements. Prior or subsequent to the measurement, in order to calculate the heat capacity of the liquid sample, the heat capacity of the empty cell was measured with a thermal radiation calorimeter that had already been developed.

The heat capacity measured with the present calorimeter seems to be close to that at constant total volume of a liquid with a small amount of its vapor or that under the saturated vapor pressure rather than that at a constant pressure, C_p. Because the vapor pressure is low for the present conditions, the measured value is assumed to be approximately equal to C_p. The temperature gradient in the radial direction of the present cell is not negligible because the thermal diffusivity of the liquid is rather small and there is the resistance to heat transfer from the cell wall to the liquid in the cell. Taking into account these points, the uncertainty of the measured C_p with the present calorimeter will be discussed in Section 3.

3. RESULTS AND DISCUSSION

In the present method, it is necessary that E_h does not change sharply and does not fluctuate in the present temperature range. It is desirable that E_h is high and remains constant in that range. For that purpose, it is required that the surfaces of the sample cell, the heater, and the wall of chamber are *gray*-like and their emissivities are high, and their variations are small over the measurement temperature range (see Appendix). To check the emissivity of the surface of the sample cell without blackening, the following experiment was performed. The normal reflection spectra, $R(\lambda)$, of the Pyrex glass used for the sample cell was measured in the wavelength range from 3 to 200 μm at room temperature using a Brucker 113v FT-IR spectrometer. The spectral emissivity, $\epsilon_\lambda(\lambda)$, assumed to be $1 - R(\lambda)$, is shown in Fig. 2a. Assuming that Lambert's law holds, the hemispherical total emissivity, $\epsilon(T)$, was estimated from

$$\epsilon = \frac{\int_{3\,\mu\mathrm{m}}^{200\,\mu\mathrm{m}} \epsilon_\lambda(\lambda)\, W(\lambda, T)\, d\lambda}{\int_{3\,\mu\mathrm{m}}^{200\,\mu\mathrm{m}} W(\lambda, T)\, d\lambda} \tag{3}$$

$$\approx \frac{\int_{3\,\mu\mathrm{m}}^{200\,\mu\mathrm{m}} \epsilon_\lambda(\lambda)\, W(\lambda, T)\, d\lambda}{\sigma T^4}, \tag{4}$$

where $W(\lambda, T)$ is Planck's emissive power. Figure 2b shows the calculated results of $\epsilon(T)$. The values of $\epsilon(T)$ calculated from Eqs. (3) and (4) are almost the same, 0.88 ± 0.01. $\epsilon(T)$ of the Pyrex glass is high and fairly constant in the temperature range from 260 to 400 K. The above result suggests that the value of E_h for the present calorimeter is almost constant in the present temperature range without blackening of the sample cell. The effective emissivity E_h was determined experimentally by measuring the specific heat of water for which the values of JSTP [10] were used. Figure 3 shows the temperature dependence of E_h. E_h is more or less constant with temperature, and its value was 0.440 ± 0.007 in the range from 280 to 360 K.

Figure 4 shows T_h and dT_s/dt versus T_s for heating and cooling processes in the present calorimeter when the sample was water. $I_\mathrm{hi} - I_\mathrm{hd}$ and $(dT_\mathrm{s}/dt)_\mathrm{i} - (dT_\mathrm{s}/dt)_\mathrm{d}$ calculated from Fig. 4 are shown in Fig. 5. $C_\mathrm{p}/E_\mathrm{h}$ can be estimated from the ratio of $I_\mathrm{hi} - I_\mathrm{hd}$ to $(dT_\mathrm{s}/dt)_\mathrm{i} - (dT_\mathrm{s}/dt)_\mathrm{d}$ at the same T_s by Eq. (2). The heat capacity of a sample is derived from $C_\mathrm{p}/E_\mathrm{h}$ and E_h.

The heat capacities of ethanol, ethylene glycol, n-heptane, and n-valeric acid (Wako Chemical Co., Japan) were measured to establish the accuracy of the present calorimeter. The purities of these samples as stated by the manufacture were 99.5, 99, 99.9, and more than 95%, respectively,

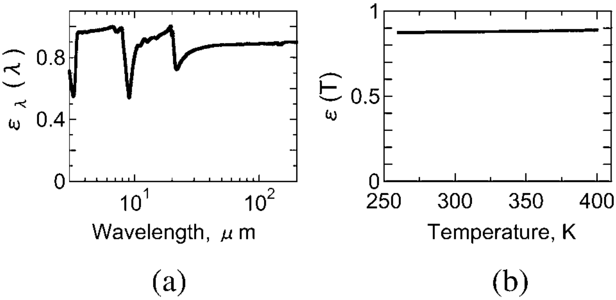

(a) (b)

Fig. 2. (a) Spectral emissivity of Pyrex glass at room temperature. (b) Hemispherical total emissivity of Pyrex glass.

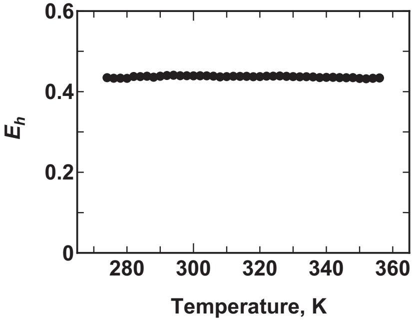

Fig. 3. Temperature dependence (280 to 360 K) of the effective emissivity E_h obtained from the experiment with water.

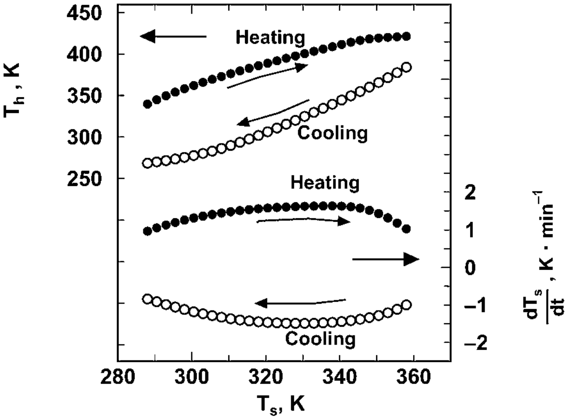

Fig. 4. dT_s/dt and T_h versus T_s for heating and cooling processes in the present calorimeter when the sample is water.

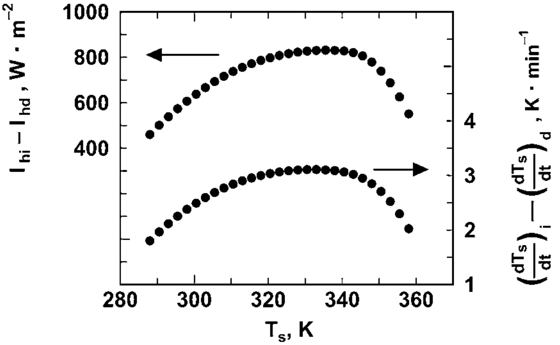

Fig. 5. $I_{hi} - I_{hd}$ and $(dT_s/dt)_i - (dT_s/dt)_d$ calculated from Fig. 4.

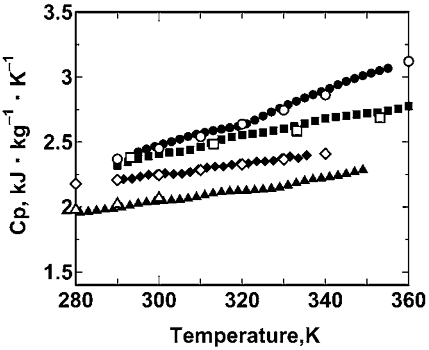

Fig. 6. Temperature dependence (280 to 360 K) of the heat capacities of several liquid samples with the thermal radiation calorimeter. The closed symbols refer to the present results. (●) ethanol, (■) ethylene glycol, (◆) n-heptane, (▲) n-valeric acid. The open symbols refer to reference data. (○) JSTP Handbook [10], (□) Stephens and Tamplin [11] (◇) Van Miltenburg et al. [12], (△) McDougall and Kilpatrick [13].

and these samples were used without further purification. These results are shown in Fig. 6. The closed symbols denote the present results, and the open symbols denote reference values from the literature (the data of JSTP [10] for ethanol, Stephens and Tamplin [11] for ethylene glycol, Van Miltenburg et al. [12] for n-heptane, and McDougall and Kilpatrick [13] for n-valeric acid). The deviations from the reference data were between −0.34 and +1.33% for ethanol, −1.68 and +1.54% for ethylene glycol, +0.22 and +0.63% for n-heptane, and −1.21 and −1.63% for n-valeric acid. The present samples of n-valeric acid and ethylene glycol were not pure enough to consider these deviations in detail, however, the results for ethanol and n-heptane indicate that the deviation of the measured heat capacities from reference data is within ±2.0% taking into account the purities.

Figure 7 shows the results of the heat capacity of water + ethanol mixtures when the mole fraction of water is 0.699 in the temperature range from 290 to 350 K. The closed circles, the open circle, and the open triangle refer to the present values, that at 298.15 K of Ogawa and Murakami [14], and that at 308.15 K of Besson and Patrick [15], respectively. The measured values were in good agreement with these reference values within ±0.6%. The excess heat capacity, C_p^{E} is defined by

$$C_p^{\mathrm{E}} = C_{p,\,\mathrm{m}} - xC_{p,\,\mathrm{w}} + (1-x)\, C_{p,\,\mathrm{et}}, \tag{5}$$

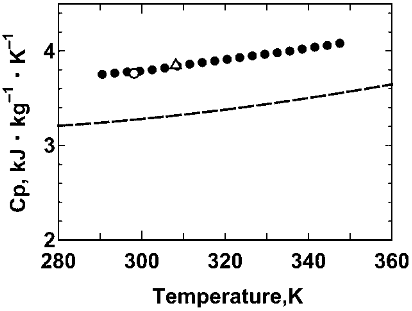

Fig. 7. Temperature dependence (290 to 350 K) of the heat capacities of water + ethanol mixtures when the mole fraction of water is 0.699. (●) Present results, (○) Ogawa and Murakami [14], (△) Besson and Patrick [15]. The dashed line represents $xC_{p,\mathrm{w}}+(1-x)\,C_{p,\mathrm{et}}$.

where $C_{p,\mathrm{m}}$ is the heat capacity of the mixture, x is the mole fraction of water in the mixture, and $C_{p,\mathrm{w}}$ and $C_{p,\mathrm{et}}$ are the heat capacities of pure water and ethanol, respectively. The dashed line in Fig. 7 indicates $xC_{p,\mathrm{w}}+(1-x)\,C_{p,\mathrm{et}}$ for the purpose of comparison. For the present case, C_p^{E} is relatively large compared with the general mixture. In the present experiment, the values of C_p^{E} are 13.3 ± 0.5 and 13.5 ± 0.5 J · mol^{-1} · K^{-1} at 298.15 and 308.15 K, respectively. These values agree to some extent with the previous data, 13.12 J · mol^{-1} · K^{-1} (298.15 K, Ogawa and Murakami [14]), and 13.78 J · mol^{-1} · K^{-1} (308.15 K, Besson and Patrick [15]).

From Eq. (2), the relative error of C_p in the present measurement can be estimated by

$$\begin{aligned}\Delta C_\mathrm{p} &= \frac{\partial C_\mathrm{p}}{\partial A}\,\Delta A+\frac{\partial C_\mathrm{p}}{\partial M}\,\Delta M+\frac{\partial C_\mathrm{p}}{\partial E_\mathrm{h}}\,\Delta E_\mathrm{h}+\frac{\partial C_\mathrm{p}}{\partial T_\mathrm{hi}}\,\Delta T_\mathrm{hi}\\ &\quad+\frac{\partial C_\mathrm{p}}{\partial T_\mathrm{hd}}\,\Delta T_\mathrm{hd}+\frac{\partial C_\mathrm{p}}{\partial \dot{T}_\mathrm{si}}\,\Delta \dot{T}_\mathrm{si}+\frac{\partial C_\mathrm{p}}{\partial \dot{T}_\mathrm{sd}}\,\Delta \dot{T}_\mathrm{sd},\end{aligned}\tag{6}$$

$$\begin{aligned}\therefore\left|\frac{\Delta C_\mathrm{p}}{C_\mathrm{p}}\right| &\leqslant \left|\frac{\Delta A}{A}\right|+\left|\frac{\Delta M}{M}\right|+\left|\frac{\Delta E_\mathrm{h}}{E_\mathrm{h}}\right|+\left|\frac{4T_\mathrm{hi}^3\Delta T_\mathrm{hi}}{T_\mathrm{hi}^4-T_\mathrm{hd}^4}\right|\\ &\quad+\left|\frac{4T_\mathrm{hd}^3\Delta T_\mathrm{hd}}{T_\mathrm{hi}^4-T_\mathrm{hd}^4}\right|+\left|\frac{\Delta \dot{T}_\mathrm{si}}{\dot{T}_\mathrm{si}-\dot{T}_\mathrm{sd}}\right|+\left|\frac{\Delta \dot{T}_\mathrm{sd}}{\dot{T}_\mathrm{si}-\dot{T}_\mathrm{sd}}\right|.\end{aligned}\tag{7}$$

The typical values of these parameters in the present study when the sample is water are as follows: $E_\mathrm{h}=0.440$, $\Delta E_\mathrm{h}=0.007$, $M=5.000$ g, $\Delta M=0.005$ g, $T_\mathrm{hi}^4-T_\mathrm{hd}^4=14\times10^9$ K^4, $4T_\mathrm{hi}^3=2.5\times10^8$ K^3, $4T_\mathrm{hd}^3=1.3\times10^8$ K^3,

$\Delta\dot{T}_s = 0.01\ \mathrm{K \cdot min^{-1}}$, $\dot{T}_{si} - \dot{T}_{sd} = 3\ \mathrm{K \cdot min^{-1}}$. The diameter of the sample cell is large so that temperature gradients in the radial direction are not negligible because the thermal diffusivity of a liquid is fairly small in comparison with that of a solid. ΔT_h is mainly caused by the non-uniform temperature profile in the cell. The following is the reason. Strictly speaking, T_s, which appears on the right-hand side of Eq. (1), is the temperature at the sample cell surface, while that on the left-hand side is the average value of the cell temperature. Equation (2) can be derived from Eq. (1) at the same temperature of the cell surface for the heating and cooling processes. However, in the present measurement, the value of T_h was taken at the same temperature of the center of the cell, at where the tip of the thermocouple was placed, for both processes. The difference between the temperature at the center of the cell and that at the cell surface when the sample is water, and $dT/dt = 1\ \mathrm{K \cdot min^{-1}}$ without convection was calculated to be 0.6 K in the present temperature range by numerical analysis. Therefore, ΔT_h is 0.6 K assuming that T_h is proportional to T_s for the case with a small variation of the absolute value of T_h and T_s. ΔA is not considered because the same sample cell was used for all measurements and the determination of E_h, so the uncertainty of A causes only a relative shift of the value of E_h. Based on the above assumption, the relative error of C_p is estimated to be less than 3.7%. In this estimation, ΔT_h strongly influences ΔC_p, therefore, the improvement of the sample cell to achieve the temperature uniformity and measurement of the temperature at the cell surface are needed.

However, the maximum deviation of the present results from the reference data seems to be somewhat smaller than the calculated relative error. This suggests the following probability. In the present method, the apparatus calibration constant E_h is estimated with the reference sample having a known heat capacity. All measurements of the heat capacities were carried out with the same apparatus and at the same conditions when the measurement of E_h was performed. This probably reduced the uncertainty of the measured values to some extent.

4. CONCLUSION

Measurement of the specific heat capacity of a liquid sample in the temperature range from 280 to 360 K was performed by an apparatus based on thermal radiation calorimetry. The present calorimeter enables the value of the heat capacity of a liquid sample to be obtained continuously with temperature. The sample cell was made of Pyrex glass. It is not necessary that the surface of the sample cell is blackened with high emissivity materials because the emissivity of Pyrex glass is very high and constant in the present temperature range. Most liquids do not react with Pyrex glass. It is an advantage for the study of the heat capacity of a liquid. Moreover, in the present method, the construction and operation of the apparatus are very simple and the specific heat can be measured in a straightforward manner and in a rather short time. In the present study, the specific heat capacities of ethanol, ethylene glycol, n-heptane, n-valeric acid, and water + ethanol mixtures were measured. The relative error of the heat capacity measured by the present calorimeter when the sample is water and $dT_s/dt = 1\ \mathrm{K \cdot min^{-1}}$ was estimated to be smaller than $\pm 3.7\%$. The maximum deviation of the measured values from the reference data was within this value. To measure the specific heat capacity of liquid samples with higher precision and sensitivity, the temperature uniformity of the sample cell, the use of pure liquids, and better stability of the radiation flux supplied to a sample are required. The continued development is proceeding.

APPENDIX

In a previous paper [8], the radiant power exchange between the sample, the heater, and the wall of the chamber when a sample is heated only on one face by a flat heater was calculated using the net-radiation method [9]. In that paper, the frustum of the right circular cone composed of only three surfaces was considered, and the interior top and base were assumed to be the sample surface facing the heater and the heater surface, respectively.

In the following, the more general expression of the total radiation energy arriving at the surface in an enclosure composed of *n* discrete surface areas is derived (see Fig. A1). These surfaces are assumed to be

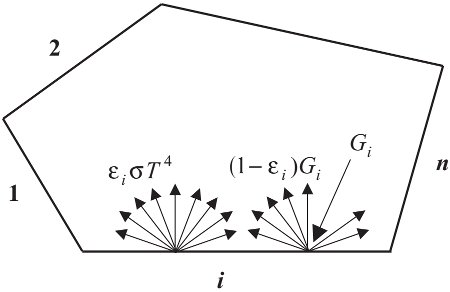

Fig. A1. Enclosure composed of *n* discrete surface areas.

diffuse and *gray*. The outgoing radiant energy flux leaving from the ith inside surface, J_i, is

$$J_i = \epsilon_i \sigma T_i^4 + (1-\epsilon_i)\, G_i = \epsilon_i I_i + (1-\epsilon_i)\, G_i, \tag{A1}$$

where I is the emissive power per unit area of blackbody radiation, which is equal to σT_i^4 (σ is the Stefan-Boltzmann constant and T_i is the temperature of the ith surface), ϵ_i is the emissivity, and G_i is the incoming radiant energy flux. The net radiation energy received by the ith inside surface, Q_i, is

$$Q_i = A_i(G_i - J_i) \qquad (A_i \text{ is the area of the } i\text{th inside surface}),$$

therefore,

$$\begin{aligned} J_i &= G_i - q_i && (q_i = Q_i/A_i) \\ \therefore J_i &= I_i + R_i q_i && (\because \text{(A1)}, R_i = (1-\epsilon_i)/\epsilon_i). \end{aligned} \tag{A2}$$

Moreover, Q_i can be written in terms of the configuration factor,

$$\begin{aligned} Q_i &= \sum_{k=1}^{n} J_k A_k F_{k-i} - J_i A_i \\ &= A_i \sum_{k=1}^{n} F_{i-k}(J_k - J_i) \\ &\left(\because A_i F_{i-k} = A_k F_{k-i}, \sum_{k=1}^{n} F_{i-k} = 1\right), \end{aligned} \tag{A3}$$

where F_{i-k} is the configuration factor which is the fraction of energy leaving from the ith surface that arrives at the kth surface. From Eqs. (A2) and (A3),

$$\begin{aligned} q_i &= \sum_{k=1}^{n} F_{i-k}(I_k - I_i + R_k q_k - R_i q_i) \\ \therefore \sum_{k=1}^{n} \{(1+R_i)\,\delta_{ik} - F_{i-k}R_k\}\, q_k &= \sum_{k=1}^{n} F_{i-k}(I_k - I_i). \end{aligned} \tag{A4}$$

The following equation is derived using Cramer's formula,

$$\begin{aligned} q_l &= \frac{1}{|\mathbf{A}|} |(\mathbf{a}_1, \mathbf{a}_2, \ldots, \mathbf{a}_{l-1}, \mathbf{c}, \mathbf{a}_{l+1}, \ldots, \mathbf{a}_n)| \\ &= \frac{1}{|\mathbf{A}|} \sum_{i=1}^{n} \tilde{\mathbf{A}}_{il} \sum_{k=1}^{n} F_{i-k}(I_k - I_i) \end{aligned}$$

$$=\frac{1}{|\mathbf{A}|}\sum_{i=1}^{n}\tilde{\mathbf{A}}_{il}\left\{\sum_{k=1}^{n}F_{i-k}(I_k-I_l)-(I_i-I_l)\right\}$$

$$\left(\because\ \sum_{k=1}^{n}F_{i-k}=1\right)$$

$$=\frac{1}{|\mathbf{A}|}\sum_{k=1}^{n}\left\{\sum_{i=1}^{n}\tilde{\mathbf{A}}_{il}(F_{i-k}-\delta_{ik})\right\}(I_k-I_l), \tag{A5}$$

where the matrix $\mathbf{A}_{ik}=(\mathbf{a}_1,\mathbf{a}_2,\ldots,\mathbf{a}_n)_{ik}=(1+R_i)\,\delta_{ik}-F_{i-k}R_k$, row vector $\mathbf{c}_i=\sum_{k=1}^{n}F_{i-k}(I_k-I_i)$, and $\tilde{\mathbf{A}}_{il}$ is a cofactor. Therefore, q_i can be expressed as

$$q_i=\sum_{k=1}^{n}E_{ik}(I_k-I_i), \tag{A6}$$

where E_{ik} is the effective emissivity given by

$$E_{ik}=\frac{1}{|\mathbf{A}|}\left\{\sum_{j=1}^{n}\tilde{\mathbf{A}}_{ji}(F_{j-k}-\delta_{jk})\right\}. \tag{A7}$$

E_{ik} depends on the geometric configuration and the emissivities of these surfaces.

In the present work, the sample cell was made of Pyrex glass. The Pyrex glass surface is assumed to reflect not diffusely but in a mirror-like manner. However, the above expression holds if the configuration factor F is replaced with the *exchange factor* F^s. F^s is the fraction of the radiant energy leaving a surface that arrives at the other surface both directly and by all possible intermediate specular reflection [9], given by

$$F^s_{1-2}=F_{1-2}+\rho_3F_{1-3-2}+\rho_4F_{1-4-2}+\cdots+\rho_3\rho_4F_{1-3-4-2}+\cdots, \tag{A8}$$

where ρ is the reflectivity.

REFERENCES

1. O. Makarounis, *Progress in Astronautics and Aeronautics* **20**:203 (1967).
2. A. Cezairliyan, M. S. Morse, H. A. Berman, and C. W. Beckett, *J. Res. Natl. Bur. Stand. A*. **75A**:65 (1970).
3. C. K. Hsieh and X. A. Wang, *Rev. Sci. Instr.* **53**:684 (1982).
4. J. Straub, A. Haupt, and K. Nitsche, *Fluid Phase Equil.* **88**:123 (1993).
5. K. Hisano and T. Yamamoto, *High Temp.-High Press.* **25**:337 (1993).
6. K. Morimoto, S. Sawai, and K. Hisano, *Int. J. Thermophys.* **20**:709 (1999).
7. S. Sawai, H. Tanaka, K. Morimoto, and K. Hisano, *Int. J. Thermophys.* **20**:721 (1999).
8. K. Hisano, S. Sawai, and K. Morimoto, *Int. J. Thermophys.* **19**:305 (1998).

9. R. Siegel and J. R. Howell, *Thermal Radiation Heat Transfer* (Taylor and Francis, Washington D.C., 1992).
10. Japan Society of Thermophysical Properties, *Thermophysical Properties Handbook* (Yokendo, Tokyo, 1990) [in Japanese].
11. M. A. Stephens and W. S. Tamplin, *J. Chem. Eng. Data* **24**:81 (1979).
12. J. C. Van Miltenburg, G. J. K. Van den Berg, and M. J. Van Bommel, *J. Chem. Thermodynamics* **19**:1129 (1987).
13. L. A. McDougall and J. E. Kilpatrick, *J. Chem. Phys.* **42**:2307 (1965).
14. H. Ogawa and S. Murakami, *Thermochimica. Acta* **109**:145 (1986).
15. G. C. Besson and J. D. Patrick, *J. Chem. Eng. Data* **27**:439 (1982).